European Review for Medical and Pharmacological Sciences 2020; 24: 9511-9521

Correlations of hsa_circ_0046264 expression with onset, pathological stage and chemotherapy resistance of lung cancer

Z.-H. LIU[1], S.-Z. YANG[1], X.-T. CHEN[1], M.-R. SHAO[1], S.-Y. DONG[1], S.-Y. ZHOU[1], L. LIU[2]

[1]Department of Thoracic Surgery, The First Affiliated Hospital of China Medical University, Shenyang, China
[2]Department of Ophthalmology, The First Affiliated Hospital of China Medical University, Shenyang, China

Abstract. – OBJECTIVE: The purpose of this study was to investigate the correlations of hsa_circ_0046264 expression with the onset, pathological stage, and chemotherapy resistance of lung cancer.

PATIENTS AND METHODS: Firstly, gene expression profiling microarrays were applied to screen the differentially expressed circular ribonucleic acids (circRNAs) in the tumor tissues of patients with non-small cell lung cancer (NSCLC). Secondly, quantitative Reverse Transcription-Polymerase Chain Reaction (RT-qPCR) assay was adopted to further verify the circRNAs with significant differences. Thirdly, the correlations of hsa_circ_0046264 expression level with the clinical features of NSCLC patients were explored *via* statistical analysis. Fourthly, Kaplan-Meier survival analysis and receiver operating characteristic (ROC) curve were utilized to investigate the influence of hsa_circ_0046264 expression level on the survival of the patients. Finally, the role of hsa_circ_0046264 in the process of lung cancer was probed using *in vitro* experimental methods.

RESULTS: It was shown in the results of gene microarray assay that hsa_circ_0046264 was the most prominently upregulated gene, and RT-qPCR assay further proved that hsa_circ_0046264 expression was upregulated remarkably in the tissues of tumor patients. Clinical analysis indicated that the expression level of hsa_circ_0046264 was notably associated with the patient's age, tumor size, tumor-node-metastasis (TNM) stage, and lymph node metastasis ($p<0.01$). In addition, Kaplan-Meier statistical analysis manifested that the patients in hsa_circ_0046264 low-expression group had a markedly longer survival than those in hsa_circ_0046264 high-expression group. In the tumor tissues and serum of the patients, the area under ROC curve of hsa_circ_0046264 was 0.971 and 0.915, the specificity was 0.973 and 0.957, and the sensitivity was 0.951 and 0.927, while the Youden Index was 0.924 and 0.884 respectively. The results of Cell Counting Kit-8 (CCK-8) assay revealed that the proliferative ability of lung cancer A549 cells was significantly enhanced at 36, 48, and 72 h in hsa_circ_0046264 overexpression group. According to the results of wound-healing assay, the migratory ability of A549 cells was distinctly strengthened in hsa_circ_0046264 overexpression group compared with that in the control group ($p<0.05$). Moreover, the transwell assay results pointed out that the invasive ability of A549 cell lines at 48 h after overexpression of hsa_circ_0046264 was evidently stronger than that in control group ($p<0.05$). Under the stimulation of different doses of cisplatin, hsa_circ_0046264 overexpression group had a clearly raised survival rate of A549 cells in comparison with control group, and the differences in data were statistically significant ($p<0.01$).

CONCLUSIONS: Hsa_circ_0046264 may serve as a potential biomarker for the diagnosis and prognosis and a possible therapeutic target of lung cancer.

Key Words:
Hsa_circ_0046264, Onset of lung cancer, Pathological stage, Chemotherapy resistance.

Introduction

Lung cancer is still one of the diseases with the highest mortality rate around the world. The morbidity rate of non-small cell lung cancer (NSCLC) accounts for 85% of all types of lung cancer[1]. NSCLC can be further divided into lung adenocarcinoma, squamous lung carcinoma, large

Corresponding Author: Lei Liu, MD; e-mail: 148035452@qq.com

cell carcinoma, and other lung cancers, among which lung adenocarcinoma has the highest morbidity and fatality rates[2]. In spite of the progress in diagnostic techniques for lung cancer and the marketing of new-generation targeted therapeutic drugs, the 5-year survival rate of the lung cancer patients remains very low, while the recurrence rate is fairly high[3]. Discovering the molecules that play vital roles in the process of lung cancer will be conducive to better understanding the mechanisms of progression, migration, and drug resistance of lung cancer, finally helping the early diagnosis of lung cancer and development of more efficacious therapeutic methods[4]. Therefore, it is an urgent need to delve deeper into the pathogenesis of lung cancer and discover novel molecular markers.

Circular ribonucleic acids (circRNAs) are a class of endogenous non-coding RNAs which possess stable molecular structures and highly specific expressions in tissues, so they can be taken as specific molecular markers[4]. Besides, circRNAs exert molecular sponge effects by negatively regulating miRNAs, thus controlling their target genes and ultimately being crucial players in relevant diseases[5]. CircRNAs play essential roles in the development of lung cancer. Notably, Jiang et al[6] proved through gene expression profile microarrays and *in vitro* experiments that hsa_circ_0007385 has the functions of proto-oncogenes in NSCLC. In addition, circRNAs can also act as therapeutic targets and potential biomarkers for patient's prognosis in the case of tumor. The expression level of circRNA_100876 is remarkably elevated in the tumor tissues of NSCLC patients compared with that in para-carcinoma tissues, and it is prominently associated with lymph node metastasis, tumor stage, and survival of the patients[7]. However, the roles of more circRNAs in lung cancer are still unknown.

In this research, the gene expression microarray was applied to screen the differentially expressed circRNAs in the tumor tissues of NSCLC patients firstly. Then, quantitative Reverse Transcription-Polymerase Chain Reaction (RT-qPCR) assay was adopted to further verify the circRNAs with significant differences. Subsequently, the correlations of hsa_circ_0046264 expression level with the clinical features of NSCLC patients were explored *via* statistical methods. Later, Kaplan-Meier survival analysis and receiver operating characteristic (ROC) curve were utilized to investigate the influence of hsa_circ_0046264 expression level on the survival of the patients. Finally, the role of hsa_circ_0046264 in the process of NSCLC was probed using *in vitro* experimental methods. The results demonstrated that hsa_circ_0046264 might serve as a latent biomarker for prognosis and a potential therapeutic target of lung cancer.

Patients and Methods

Collection of Tissue Samples

A total of 61 cases of tumor tissues and para-carcinoma tissues were obtained from tumor samples excised *via* operation in our hospital from April 2018 to December 2018. After resection of tumor samples, the tumor tissues and para-carcinoma tissues were immediately placed in RNA fixer reagent (Bioteke, Beijing, China) and stored in a refrigerator at -80°C until use. To exclude the factors affecting the expression profile of circRNAs, the participants who received no drug therapies before operation, including chemotherapy, radiotherapy, and targeted therapeutic drugs, were excluded in this research. All the tissue samples were confirmed as tumor tissues or para-carcinoma tissues of NSCLC by histomorphology. This study was approved by the Ethics Committee of The First Affiliated Hospital of China Medical University. Signed written informed consents were obtained from all participants before the study.

Gene Microarray Assay

Total RNAs were extracted from MGC-803 cells and MGC-803/MTA cells, and then, quantified using NanoDrop kit (Thermo Fisher, Waltham, MA, USA). Next, the integrity of the RNAs was evaluated by Bioanalyzer 2100 (Agilent, Santa Clara, CA, USA). In this research, Affymetrix 3' IVT Express kit and 100 ng of total RNAs were applied to prepare cRNA, which was hybridized on the Affymetrix PrimeView Human Array at 45°C for 16 h, according to the user manual of GeneChip 3' Array (Affymetrix, Santa Clara, CA, USA). In addition, the array was processed on the Affymetrix FS-450 Fluidics Station for washing, staining, and scanning using the Affymetrix GeneChip Scanner (Affymetrix, Santa Clara, CA, USA) in accordance with the manufacturer's protocol. The raw data in the CEL files were imported into Partek Genomics Suite 6.6 software, and the probe sets were standardized by Robust Multi-array Average method. Finally, one-way analysis of variance was adopted to determine the significance of the

differentially expressed genes, and *p*-values were corrected by FDR.

qRT-PCR Assay

qRT-PCR were employed to detect the expressions. The tissue samples were taken out from cryogenic tubes, drained, and ground in liquid nitrogen in 5 mL tubes. After thorough homogenization in a tissue homogenizer, the liquid was transferred into clean imported Eppendorf (EP; Hamburg, Germany) tubes (1.5 mL) and placed at room temperature for 5-10 min for adequate lysis, followed by centrifugation at 1,200 rpm for 5 min. Then, the precipitate was discarded, and chloroform (200 μL chloroform/mL TRIzol) was added, mixed by shaking, placed at room temperature for 15 min, and centrifuged at 12,000 rpm and 4°C for 15 min. After that, the supernatant was absorbed into another centrifuge tube and added with isopropyl alcohol (0.7-1 time of absorbed supernatant in volume), followed by placing at room temperature for 10-30 min and centrifugation at 12000 rpm for 10 min. After the supernatant was discarded, the RNA was precipitated at the bottom of the tube. Subsequently, 75% ethanol (1 mL 75% ethanol/TRIzol) was added, and the centrifuge tube was shaken gently to suspend the precipitate, followed by centrifugation at 4°C and 12,000 rpm for 5 min. The supernatant was discarded as much as possible, and the samples were blown dry on a super-clean bench for 10-20 min. Later, 10-50 μL of DEPC-treated ddH_2O was added to dissolve the precipitate, and the concentration was measured using an OneDrop micro-spectrophotometer. After that, RT reaction was conducted under the conditions of 4.5 μL of RNase free ddH_2O, 2 μL of 5 × RT reaction buffer, 0.5 μL of Random primer, 0.5 μL of Oligo(dT), 0.5 μL of reverse transcriptase, and 2 μL of RNA. The complementary deoxyribonucleic acid (cDNA) samples were assigned into three parts, each of which was diluted at 1:20. Then, 3 μL of cDNA was taken for qRT-PCR amplification. After that, 5% agarose gel electrophoresis was performed to verify the amplification level of target genes. LabWorks 4.0 image acquisition and analysis software was used for data quantification and processing. The samples in each group were measured three times to obtain reliable data. In this research, $2^{-\Delta\Delta Ct}$ method was adopted to analyze the changes in the relative expressions of target genes, and the primers utilized were synthesized by Shanghai Generay Biotech Co, Ltd. (Shanghai, China). Primers used were shown in Table I.

Cell Culture

Human NSCLC cell line A549 was purchased from the Institute of Microbiology, Chinese Academy of Sciences (Beijing, China), phosphate-buffered saline (PBS), trypsin, fetal bovine serum (FBS), Roswell Park Memorial Institute-1640 (RPMI-1640) medium from Gibco Company (Rockville, MD, USA), and small interfering RNA (siRNA) from Guge Bio-Technology Co., Ltd. (Wuhan, China). The cells were cultured in a cell incubator with 5% CO_2 at 37°C, and they were subjected to digestion and subculture with 0.25% trypsin-EDTA (ethylenediaminetetraacetic acid) after the culture dish was fully covered with the cells.

Cell Transfection

CircRNA_0030741 was knocked down by siRNA (shRNA, Qiagen, Cambridge, MA, USA), and the circRNA_0030741-targeting siRNA (30 nM) was transfected into the cardiomyocytes of rats using the Lipofectamine 2000™ transfection reagent (Invitrogen, Carlsbad, CA, USA). 6 h later, the medium containing the transfection reagent was discarded, and the rat primary neuronal cells were further cultured in a fresh medium for 48 h.

Table I. Primer sequences.

Name	Gene	Primer sequence
Hsa_circ_0046264	Forward	5'-CGACAAAGATGGGGTTGTCC-3'
	Reverse	5'-CCAACCTGATCTCGGAACCT-3'
Hsa_circ_0030741	Forward	5'-TCGTGTCTTGTGT-TGCAGC-3'
	Reverse	5'-GTGCAGGGTCCGAGGT-3'
Hsa_circ_0000463	Forward	5'-GGCCTGAAGTGATCTAAAGG-3'
	Reverse	5'-GTATCCAGTGCGAATACCTC-3'
U6	Forward	5'-CTCGCTTCGGCAGCACA-3'
	Reverse	5'-AACGCTTCACGAATTTGCGT-3'

Detection of Impact of Hsa_circ_0046264 Expression on NSCLC Cell Proliferation Via Cell Counting Kit-8 (CCK-8)

A549 cells in the logarithmic growth phase were evenly seeded into a 96-well plate (1×10^4 cells/well), and MTA of varying diluted concentrations was added into the culture wells, with 6 wells repeated for each concentration gradient. Then, the cells were cultured in the incubator for another 72 h, the original medium was discarded, 20 μL of CCK-8 reaction solution (Dojindo, Molecular Technologies, Kumamoto, Japan), 170 μL of cell culture fluid were added, and the cells were incubated at 37°C in the dark for 2 h. Subsequently, the cells were shaken on a micro vibrator for 3 min, and the absorbance at the wavelength of 450 nm was measured using a microplate reader.

Wound-Healing Assay

The cells in the logarithmic growth phase were inoculated into the 96-well plates, ensuring that the number of cells in each plate was about 5×10^4. At 24 h, a wound was scratched in the middle of the well plate using the pipette tip, the scratched cells were washed away with PBS, and the medium was replaced with serum-free medium. Then, the cell migration was photographed and recorded under a high-power microscope at 24 h.

Transwell Assay

The transwell chambers (8 μm) were coated with Matrigel diluted at 1:8 and then incubated at 37°C for 2 for gelation. Later, A549 cells were diluted into single-cell suspension by serum-free medium and then seeded into the upper transwell chamber (5×10^4 cells/100 μL). The medium containing 10% FBS was added into the lower chamber, and the transmembrane cells were fixed in 5% glutaraldehyde after 48 h of culture, stained with 0.1% crystal violet, and photographed.

5-Ethynyl-2′-Deoxyuridine (EdU) Staining

At 24 h after overexpression of vector and circRNA, the Click-iT EdU staining kit (Invitrogen, Carlsbad, CA, USA) was applied to stain the A549 cells according to the specific procedures in the kit instructions. After that, the cells were photographed using a fluorescence microscope, and 3 fields of vision were randomly selected on each slide. Finally, the EdU-positive cells were counted.

Statistical Analysis

All the data were presented as mean ± standard deviation, the non-paired Student's *t*-test, and one-way analysis of variance were used for statistical analysis between two groups. The Statistical Product and Service Solutions (SPSS) 17.0 (SPSS Inc., Chicago, IL, USA) was employed for the statistical analysis in this research. The ROC curves and Kaplan-Meier method with the log-rank test were used for the survival analysis. $p<0.05$ suggested that the difference was statistically significant.

Results

CircRNAs with Differential Expressions in NSCLC Patients Screened Via Expression Profiles

The screening results of expression profiles showed that there were significant differences in the expression profiles of circRNAs in tumor tissues and para-carcinoma tissues of NSCLC patients (Figure 1). It was also indicated that a total of 72 circRNAs in tumor tissues exhibited significant differences compared with those in para-carcinoma tissues (fold change >2, $p<0.01$), among which the expression profiles of circRNAs were markedly upregulated in 31 cases but notably downregulated in 41 cases.

Expression Differences in CircRNAs Verified Via RT-qPCR

Considering the reliability of high-throughput screening, 3 significantly upregulated circRNAs (hsa_circ_0046264, hsa_circ_0030741 and hsa_circ_0000463) were selected for further verification by means of more reliable qRT-PCR assay. The results pointed out that the expression level of hsa_circ_0046264 was increased the most evidently in 61 cases of tumor tissues in comparison with that in para-carcinoma tissues, with statistically significant differences ($p<0.01$). Compared with para-carcinoma tissues, tumor tissues displayed significant differences in the expression levels of hsa_circ_0030741 and hsa_circ_0000463 ($p<0.05$). The research results illustrated that the tumor tissues had the most prominently elevated expression level of hsa_circ_0046264 (Figure 2). Therefore, it was assumed that hsa_circ_0046264 plays an important role in the pathological process of lung cancer, so it was selected as the object for in-depth study.

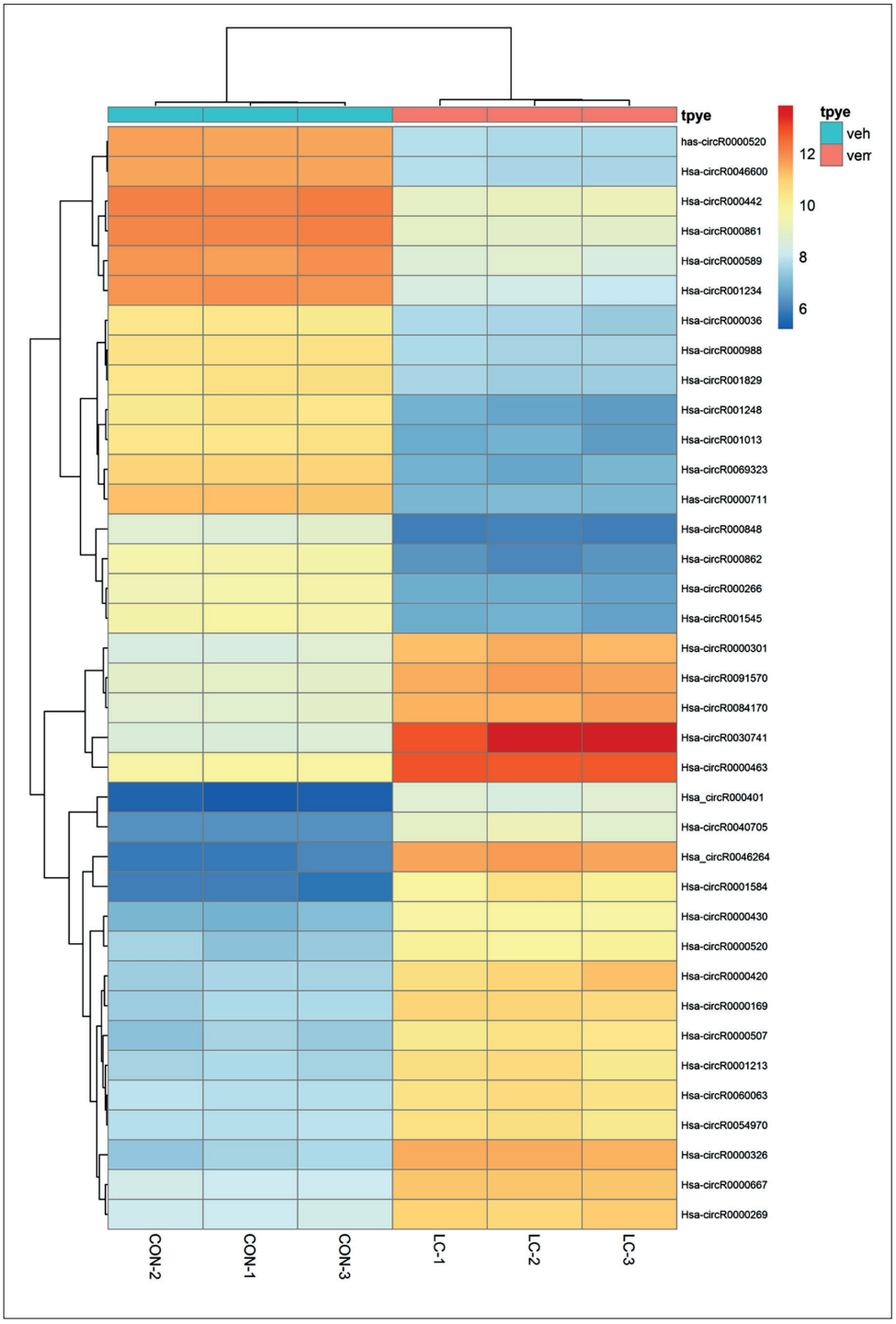

Figure 1. Differentially expressed circRNAs in tumor tissues and para-carcinoma tissues of NSCLC patients. Heatmap of unsupervised clustering analysis manifests that there are significant differences in the expression profiles of circRNAs in tumor tissues and para-carcinoma tissues of NSCLC, where LC stands for lung cancer tissues and Con for normal tissues. Each row represents a circRNA, the red color represents a high expression level and the blue represents a low expression level.

Significant Correlations of Hsa_circ_0046264 Expression Level with Clinical Features of NSCLC

Later, the correlations of hsa_circ_0046264 expression level with clinical features of NSCLC patients were analyzed. As shown in Table II, the expression level of hsa_circ_0046264 was distinctly associated with the patient's age, tumor size, tumor-node-metastasis (TNM) stage, and lymph node metastasis ($p<0.01$). However, no apparent correlation between hsa_circ_0046264 expression level and the gender of the patients was observed ($p>0.01$). Moreover, log-rank statistical analysis manifested that the

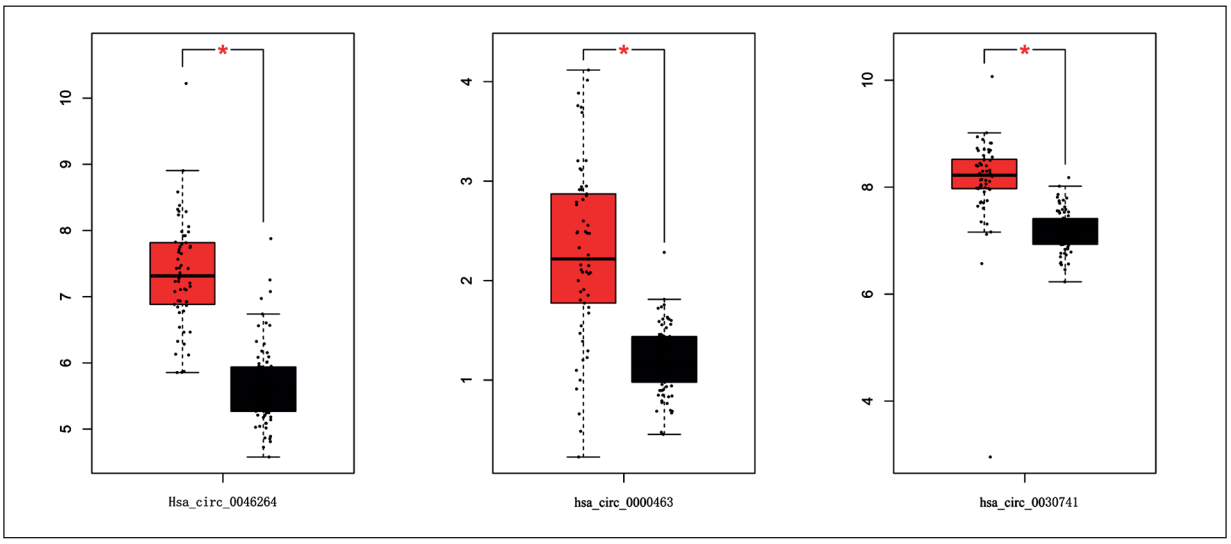

Figure 2. Differences in expression levels of hsa_circ_0046264, hsa_circ_0000520 and hsa_circ_0004018 in tumor tissues and para-carcinoma tissues detected *via* RT-qPCR assay. *$p<0.05$ *vs.* control group.

patients in hsa_circ_0046264 low expression group had a markedly longer survival than those in hsa_circ_0046264 high expression group (Figure 3).

Diagnostic Value of Hsa_circ_0046264 in NSCLC Patients

Subsequently, the sensitivity and specificity of hsa_circ_0046264 in diagnosing NSCLC were analyzed using the ROC curve (Figure 4). In the tumor tissues and serum of the patients, the area under ROC curve of hsa_circ_0046264 was 0.971 and 0.915, the specificity was 0.973 and 0.957, and the sensitivity was 0.951 and 0.927, the Youden Index was 0.924 and 0.884, respectively, indicating that the difference in the expression level of hsa_circ_0046264 is of clinical significance in diagnosing NSCLC. Hence, the expression level of hsa_circ_0046264 can help diagnose NSCLC and monitor the efficacy of medicines in NSCLC patients.

Impact of Hsa_circ_0046264 Expression Level on NSCLC Cell Proliferation

The results of CCK-8 assay revealed that the proliferative ability of lung cancer A549 cells

Table II. Correlations of hsa_circ_0046264 expression level with clinical features of NSCLC.

Clinical feature	N	Hsa_circ_0046264		*p*-value
		Low expression group	High expression group	
Age				0.03
≤ 60 years old	27	21	7	
≥ 60 years old	34	11	23	
Gender				0.547
Male	33	16	17	
Female	28	15	13	
Tumor size				0.017
< 3 cm	39	23	16	
≥ 3 cm	22	7	15	
Tumor stage				0.015
I-II	30	21	9	
III-IV	31	6	25	
Lymph node metastasis				0.004
Yes	25	19	6	
No	36	11	25	

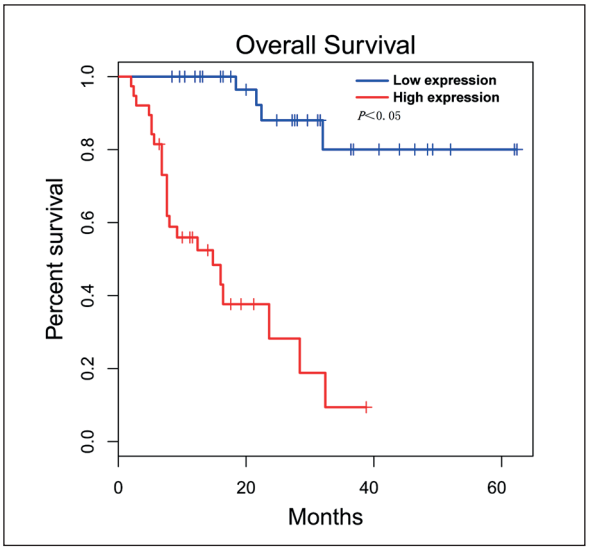

Figure 3. Impact of hsa_circ_0046264 expression level on survival of patients. Impact of hsa_circ_0046264 expression level on survival of patients analyzed through log-rank statistical analysis.

was enhanced remarkably at 36, 48, and 72 h in hsa_circ_0046264 overexpression group, suggesting that hsa_circ_0046264 can promote the proliferation of lung cancer cells (p<0.05) (Figure 5A). Furthermore, it was observed in the EdU staining results that the number of red fluorescence was increased evidently at 72 h after overexpression of hsa_circ_0046264 in comparison with that in control group, implying that hsa_circ_0046264 expression is capable of facilitating the proliferation of lung cancer cells (p<0.05) (Figure 5B).

Impacts of Hsa_circ_0046264 Expression Level on NSCLC Cell Migration and Invasion

According to the results of wound-healing assay, the migratory ability of NSCLC A549 cells was distinctly strengthened in hsa_circ_0046264 overexpression group compared with that in the control group (p<0.05), illustrating that hsa_circ_0046264 can effectively enhance the migratory ability of A549 cells (Figure 6A).

Transwell assay was employed to further assess the influence of overexpressed hsa_circ_0046264 on the invasive ability of NSCLC A549 cells, and the results manifested that the invasive ability of A549 cell lines at 48 h after overexpression of hsa_circ_0046264 was evidently stronger than that in the control group (Figure 6B).

Impact of Hsa_circ_0046264 Expression Level on Drug Resistance of NSCLC Cells

Under the stimulation of different doses of cisplatin, hsa_circ_0046264 overexpression group had a clearly raised survival rate of A549 cells in comparison with control group, and the differences in data were statistically significant (p<0.01) (Figure 7).

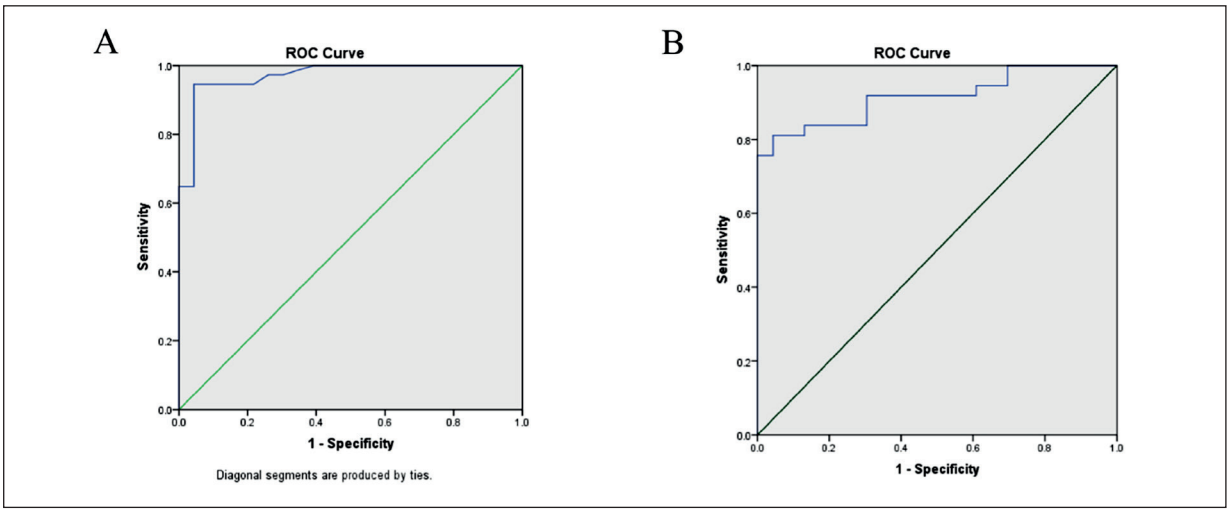

Figure 4. Specificity and sensitivity of hsa_circ_0046264 expression level as a novel NSCLC biomarker analyzed by means of ROC curve. **A,** Specificity and sensitivity of hsa_circ_0046264 expression level in the serum as a novel NSCLC biomarker analyzed via ROC curve. **B,** Specificity and sensitivity of hsa_circ_0046264 expression level in the tumor tissues as a new NSCLC biomarker analyzed by ROC curve.

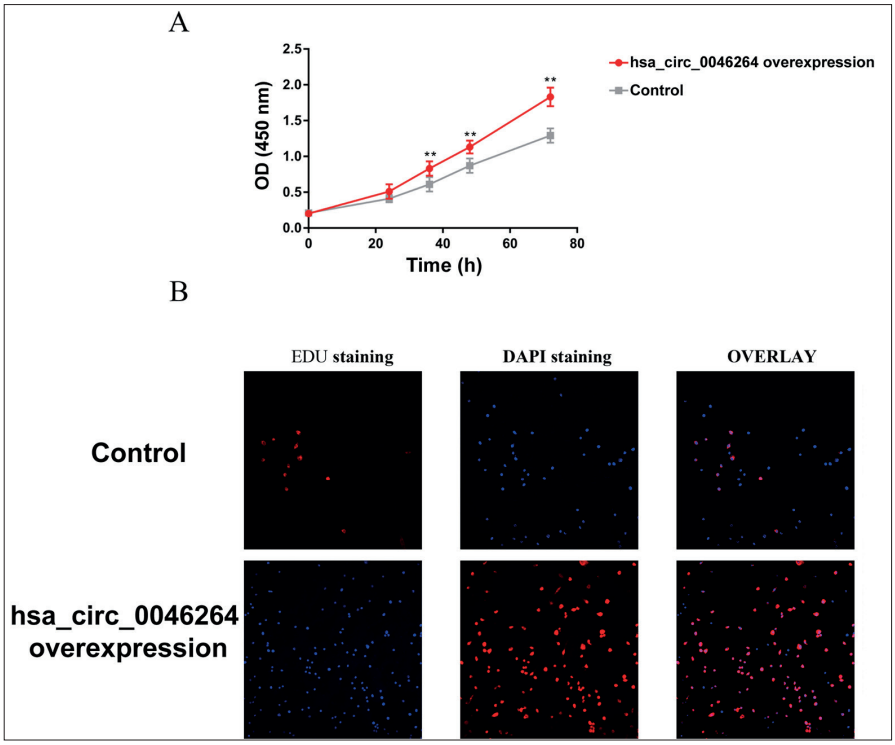

Figure 5. Impact of hsa_circ_0046264 expression level on A549 cell proliferation. **A,** Impact of hsa_circ_0046264 expression level on A549 cell proliferation detected *via* CCK-8. **B,** Impact of hsa_circ_0046264 expression level on A549 cell proliferation determined by EdU staining. **$p<0.05$ *vs.* control group (×100).

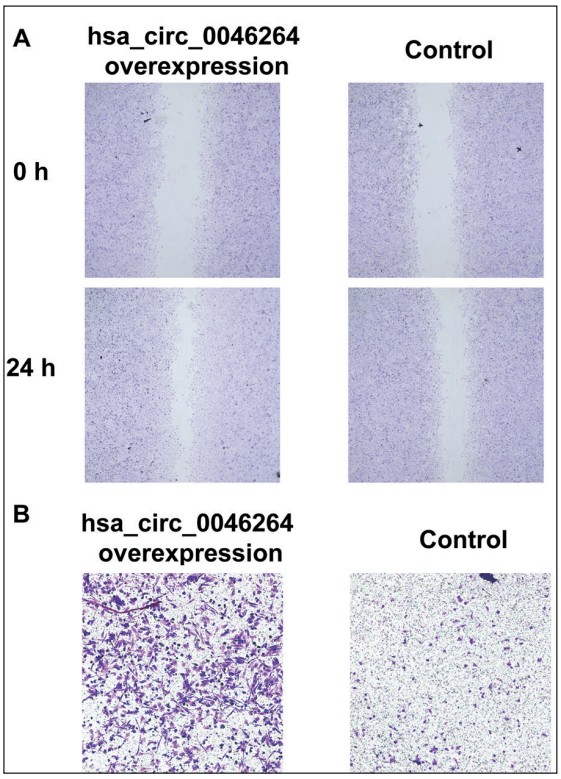

Figure 6. Impacts of hsa_circ_0046264 expression level on migration and invasion of A549 cells. **A,** Impact of hsa_circ_0046264 expression level on A549 cell migration tested through wound-healing assay (×10). **B,** Impact of hsa_circ_0046264 expression level on A549 cell invasion examined by transwell assay (×40).

Genome Ontology (GO) and Kyoto Encyclopedia of Genes and Genomes (KEGG) Enrichment Analyses

Based on the results of GO enrichment analysis, the differentially expressed genes in hsa_circ_0046264 expression group were remarkably enriched in the proliferation, proliferation regulation, migration, cycle and adhesion of A549 cells (Figure 8A). KEGG enrichment analysis revealed that the genes with differential expressions in A549 cells in hsa_circ_0046264 expression group were notably enriched in the transforming growth factor-beta (TGF-β), Wnt, phosphatidylinositol 3-kinase (PI3K)/Akt and cancer signaling pathways (Figure 8B).

Discussion

CircRNAs are a category of highly conserved non-coding RNAs that are extensively expressed in mammals. The latest studies have manifested that circRNAs play crucial roles in such processes as proliferation, differentiation, and metastasis of tumor cells. So, Hsiao et al[8] studied and proposed that circRNA_CCDC66 is a vital player in the proliferation and metastasis of colon cancer cells. Zhong et al[9] indicated that circRNA_MYLK regulates the progression of blad-

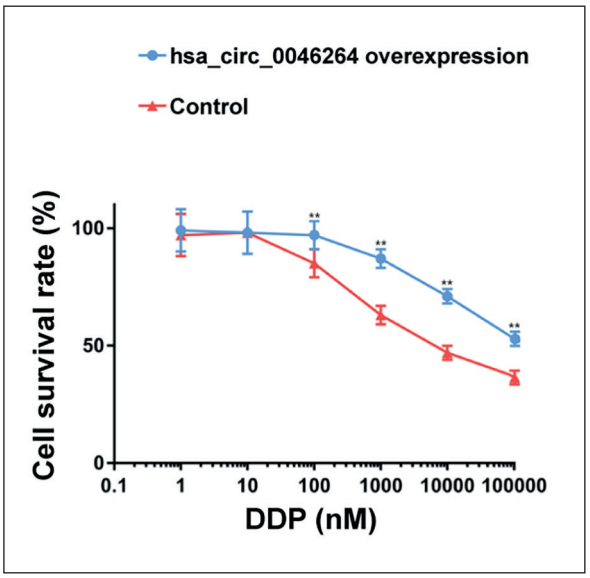

Figure 7. Impact of hsa_circ_0046264 expression level on drug resistance of A549 cells. Impact of hsa_circ_0046264 expression level on drug resistance of A549 cells detected *via* CCK-8 assay. $^{**}p<0.05$ *vs.* control group.

der cancer by modulating the VEGFA/VEGFR2 signaling pathway. Besides, Luo et al[10] illustrated that hsa_circ_0000064 is able to stimulate the proliferation and metastasis of lung cancer. All these findings elaborate that circRNAs play important roles in the occurrence and development of tumors.

During the clinical treatment of lung cancer, the early diagnosis of the disease has great effects on the treatment success rate and prognosis. Recently, a growing number of studies have pointed out that as the key regulators of lung cancer, the attention of the researchers has been paid to circRNAs. Zhang et al[11] proposed through investigations at the transcriptomic level that hsa_circ_0014130 can serve as a potential biomarker for the early diagnosis of lung cancer. In addition, Liu et al[12] researched and found that hsa_circ_0023404 promotes proliferation, migration, and invasion in NSCLC by regulating miR-217/ZEB1 axis. Despite a large number of studies, the physiological functions of a great number of circRNAs in lung cancer have not been clarified yet.

The genome-wide screening methods, including gene microarrays, are powerful experimental means for exploring pathogenic genes and possible molecular mechanisms. In this research, the differentially expressed circRNAs in the tumor tissues and para-carcinoma tissues of tumor patients were screened by means of gene microarray assay, among which hsa_circ_0046264 was upregulated the most remarkably. Next, qRT-PCR assay was performed to further testify that the hsa_circ_0046264 expression level was evidently upregulated in the tissues of tumor patients. According to the clinical analysis, the expression level of hsa_circ_0046264 had apparent associations with the age, tumor size, TNM stage, and lymph node metastasis of the patients ($p<0.01$), while it had no significant correlation with the gender of the patients ($p>0.01$). In addition, Kaplan-Meier statistical analysis manifested that the survival of the patients in hsa_circ_0046264 low expression group was markedly longer than that in hsa_circ_0046264 high expression group. In-depth analyses showed that the area under

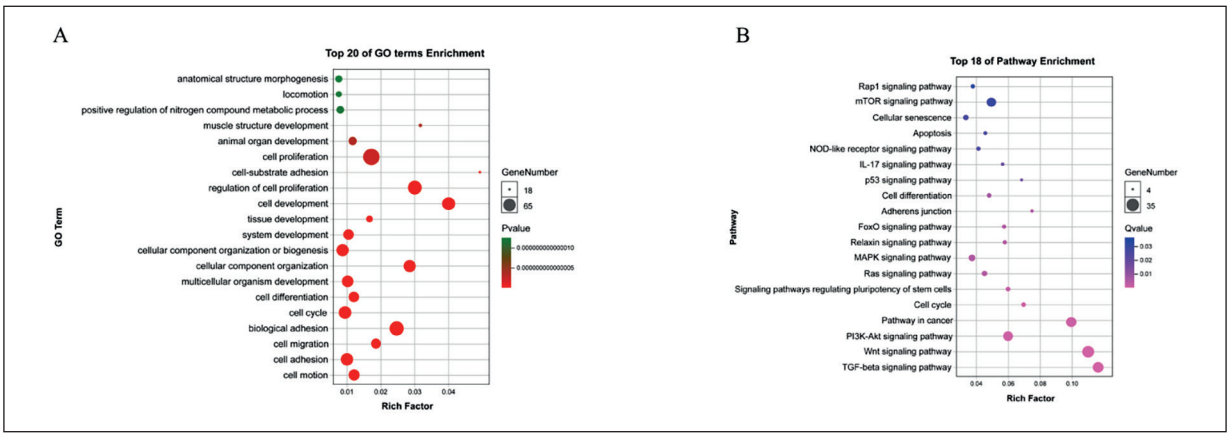

Figure 8 Bioinformatics analysis of differentially expressed genes in A549 cells in hsa_circ_0046264 expression group. **A,** GO enrichment analysis of differentially expressed genes in A549 cells in hsa_circ_0046264 expression group. **B,** KEGG enrichment analysis of differentially expressed genes in A549 cells in hsa_circ_0046264 expression group.

ROC curve of hsa_circ_0046264 was 0.971 and 0.915, the specificity was 0.973 and 0.957, and the sensitivity was 0.951 and 0.927, while the Youden Index was 0.924 and 0.884, respectively, in the tumor tissues and serum of the patients, indicating that the difference in the expression level of hsa_circ_0046264 has clinical significance in diagnosing NSCLC. Hence, the expression level of hsa_circ_0046264 can assist the diagnosis of NSCLC and monitoring of the efficacy of medicines in NSCLC patients.

It was reported in this research for the first time that hsa_circ_0046264 can be taken as a biomarker for the diagnosis and prognosis of lung cancer patients, so its role in lung cancer still remains unknown. The subsequent functional experiments revealed that hsa_circ_0000064 is capable of notably promoting the proliferation, migration, and invasion of A549 cells and distinctly improving the chemotherapy resistance of A549 cells. All these results manifest that the overexpression of hsa_circ_0046264 can lead to the phenotype of malignant tumor cells in lung cancer cells. Nevertheless, why hsa_circ_0000064 can lead to such a phenotype is still unclear.

According to the microarray results and GO for differentially expressed genes *via* DAVID database, the differentially expressed genes in hsa_circ_0046264 expression group were significantly enriched in the proliferation, proliferation regulation, migration, cycle, and adhesion of A549 cells, which were confirmed by experiments in this research. Moreover, the KEGG enrichment analysis based on KOBAS database revealed that the genes with differential expressions in A549 cells in hsa_circ_0046264 expression group were enriched in the TGF-β, Wnt, PI3K/Akt, and cancer signaling pathways the most notably. Large quantities of investigations have demonstrated that the TGF-β and Wnt signaling pathways participate in controlling endothelial-mesenchymal transition, thus facilitating the metastasis and invasion of lung cancer cells. Therefore, the enhanced migratory and invasive ability of A549 cells induced by hsa_circ_0046264 may be related to the abnormal expression of the TGF-β and Wnt signaling pathways[13-15]. Furthermore, numerous research results[16-18] have elucidated that the disorder of the PI3K/Akt signaling pathway probably causes drug resistance, as well as enhancement of proliferative signals and anti-apoptosis ability of lung cancer cells[16-18]. The in-depth experimental studies on the molecular mechanism are underway.

Conclusions

In summary, the expression level of hsa_circ_0046264 is strengthened prominently in the tissues of lung cancer patients, which is clearly correlated with the TNM stage, tumor size, lymph node metastasis, and survival rate of the disease. Besides, elevating the expression level of hsa_circ_0046264 can remarkably improve the proliferative, migratory, and invasive ability and drug resistance of lung cancer cells. These results illustrate that hsa_circ_0046264 can act as a latent biomarker for diagnosis and prognosis and a therapeutic target of lung cancer.

Conflict of Interest

The Authors declare that they have no conflict of interests.

References

1) Garon EB, Rizvi NA, Hui R, Leighl N, Balmanoukian AS, Eder JP, Patnaik A, Aggarwal C, Gubens M, Horn L, Carcereny E, Ahn MJ, Felip E, Lee JS, Hellmann MD, Hamid O, Goldman JW, Soria JC, Dolled-Filhart M, Rutledge RZ, Zhang J, Lunceford JK, Rangwala R, Lubiniecki GM, Roach C, Emancipator K, Gandhi L. Pembrolizumab for the treatment of non-small-cell lung cancer. N Engl J Med 2015; 372: 2018-2028.

2) Rizvi NA, Hellmann MD, Snyder A, Kvistborg P, Makarov V, Havel JJ, Lee W, Yuan J, Wong P, Ho TS, Miller ML, Rekhtman N, Moreira AL, Ibrahim F, Bruggeman C, Gasmi B, Zappasodi R, Maeda Y, Sander C, Garon EB, Merghoub T, Wolchok JD, Schumacher TN, Chan TA. Cancer immunology. Mutational landscape determines sensitivity to PD-1 blockade in non-small cell lung cancer. Science 2015; 348: 124-128.

3) Liu L, Zhou XY, Zhang JQ, Wang GG, He J, Chen YY, Huang C, Li L, Li SQ. LncRNA HULC promotes non-small cell lung cancer cell proliferation and inhibits the apoptosis by up-regulating sphingosine kinase 1 (SPHK1) and its downstream PI3K/Akt pathway. Eur Rev Med Pharmacol Sci 2018; 22: 8722-8730.

4) Hu J, Li P, Song Y, Ge YX, Meng XM, Huang C, Li J, Xu T. Progress and prospects of circular RNAs in Hepatocellular carcinoma: novel insights into their function. J Cell Physiol 2018; 233: 4408-4422.

5) de Oliveira JC, Oliveira LC, Mathias C, Pedroso GA, Lemos DS, Salviano-Silva A, Jucoski TS, Lobo-Alves SC, Zambalde EP, Cipolla GA, Gradia DF. Long non-coding RNAs in cancer: another layer of complexity. J Gene Med 2019; 21: e3065.

6) Jiang MM, Mai ZT, Wan SZ, Chi YM, Zhang X, Sun BH, Di QG. Microarray profiles reveal that circular RNA hsa_circ_0007385 functions as an oncogene in non-small cell lung cancer tumorigenesis. J Cancer Res Clin Oncol 2018; 144: 667-674.

7) Yao JT, Zhao SH, Liu QP, Lv MQ, Zhou DX, Liao ZJ, Nan KJ. Over-expression of CircRNA_100876 in non-small cell lung cancer and its prognostic value. Pathol Res Pract 2017; 213: 453-456.

8) Hsiao KY, Lin YC, Gupta SK, Chang N, Yen L, Sun HS, Tsai SJ. Noncoding effects of circular RNA CCDC66 promote colon cancer growth and metastasis. Cancer Res 2017; 77: 2339-2350.

9) Zhong Z, Huang M, Lv M, He Y, Duan C, Zhang L, Chen J. Circular RNA MYLK as a competing endogenous RNA promotes bladder cancer progression through modulating VEGFA/VEGFR2 signaling pathway. Cancer Lett 2017; 403: 305-317.

10) Luo YH, Zhu XZ, Huang KW, Zhang Q, Fan YX, Yan PW, Wen J. Emerging roles of circular RNA hsa_circ_0000064 in the proliferation and metastasis of lung cancer. Biomed Pharmacother 2017; 96: 892-898.

11) Zhang S, Zeng X, Ding T, Guo L, Li Y, Ou S, Yuan H. Microarray profile of circular RNAs identifies hsa_circ_0014130 as a new circular RNA biomarker in non-small cell lung cancer. Sci Rep 2018; 8: 2878.

12) Liu C, Zhang Z, Qi D. Circular RNA hsa_circ_0023404 promotes proliferation, migration and invasion in non-small cell lung cancer by regulating miR-217/ZEB1 axis. Onco Targets Ther 2019; 12: 6181-6189.

13) Zhang J, Tian XJ, Xing J. Signal transduction pathways of EMT induced by TGF-beta, SHH, and WNT and their crosstalks. J Clin Med 2016; 5. pii: E41.

14) Funaki S, Shintani Y, Kawamura T, Kanzaki R, Minami M, Okumura M. Chemotherapy enhances programmed cell death 1/ligand 1 expression via TGF-beta induced epithelial mesenchymal transition in non-small cell lung cancer. Oncol Rep 2017; 38: 2277-2284.

15) Xiao C, Wu CH, Hu HZ. LncRNA UCA1 promotes epithelial-mesenchymal transition (EMT) of breast cancer cells via enhancing Wnt/beta-catenin signaling pathway. Eur Rev Med Pharmacol Sci 2016; 20: 2819-2824.

16) Riquelme E, Behrens C, Lin HY, Simon G, Papadimitrakopoulou V, Izzo J, Moran C, Kalhor N, Lee JJ, Minna JD, Wistuba II. Modulation of EZH2 expression by MEK-ERK or PI3K-AKT signaling in lung cancer is dictated by different KRAS oncogene mutations. Cancer Res 2016; 76: 675-685.

17) Tripathi SC, Fahrmann JF, Celiktas M, Aguilar M, Marini KD, Jolly MK, Katayama H, Wang H, Murage EN, Dennison JB, Watkins DN, Levine H, Ostrin EJ, Taguchi A, Hanash SM. MCAM mediates chemoresistance in small-cell lung cancer via the PI3K/AKT/SOX2 signaling pathway. Cancer Res 2017; 77: 4414-4425.

18) Yuge K, Kikuchi E, Hagiwara M, Yasumizu Y, Tanaka N, Kosaka T, Miyajima A, Oya M. Nicotine induces tumor growth and chemoresistance through activation of the PI3K/Akt/mTOR pathway in bladder cancer. Mol Cancer Ther 2015; 14: 2112-2120.